Ionic Liquids: Ion Mobilities, Glass Temperatures, and Fragilities

Wu Xu,[†] Emanuel I. Cooper,[‡,§] and C. Austen Angell*[,†,‡]

Department of Chemistry and Biochemistry, Arizona State University, Tempe, Arizona 85287-1604, and Department of Chemistry, Purdue University, Lafayette, Indiana 87907

Received: December 1, 2002; In Final Form: March 28, 2003

We combine old, unpublished data on ionic liquids containing quaternary ammonium cations with new data on salts of aromatic cations containing a variety of anions, to demonstrate the existence for ionic liquids of an unexpectedly wide range of liquid fragilities. The pattern is one now familiar for other liquids. Here, the pattern is important in determining the relative fluid properties at ambient temperatures. We find that the optimization of ionic liquids for ambient temperature applications requiring low-vapor-pressure fluid phases involves the proper interplay of both cohesive energy and fragility factors. The cohesive energy is discussed in terms of the coulomb and van der Waals contributions to the attractive part of the pair potential. On the basis of the relation between the glass-transition temperature and the molar volume for salts with less-polarizable anions, we find evidence for a broad minimum in the ionic liquid cohesive energy at an internuclear separation of ca. 0.6 nm. This minimum lies between those of the BF_4^- and $TFSI^-$ anions for the small quaternary ammonium cations of this study. The minimum is expected to be narrower and less well-defined for salts with polarizable anions. The relation of fluidity to conductance is considered in terms of a Walden plot that is shown to provide a useful basis for organizing the observations on ionic liquids and solutions. Low vapor pressure and ideal Walden products are intimately related.

Introduction

At the present time, there is much interest in ambient-temperature liquids that consist only of cations and anions. These are known variously as "room temperature molten salts" (RTMSs), "ambient temperature melts" (ATMs), or, alternatively and increasingly, simply as "ionic liquids" (ILs). Relative to common ambient-temperature liquids and solvent mixtures, these liquids are distinguished by the fact that they do not evaporate. This renders them particularly suitable for several applications in which loss of liquid to the vapor phase constitutes a performance limitation and, often, a health hazard. The physics of ionic liquids to this point has been developed in a very empirical fashion.

The first ionic liquid was reported almost a century ago by Walden,[1] who protonated ethylamine with nitric acid (HNO_3) to yield ethylammonium nitrate, which has a melting point of $T_m = 14$ °C. Since that time, a succession of (i) viscous, water-stable, ionic liquids,[2−4] (ii) highly fluid, but water-unstable (hepta- and tetra-chloroaluminate, and chloroferrate) liquids,[5−8] and, finally, (iii) both fluid and water-stable (mostly fluorinated anion) liquids have been discovered. It is the latter cases that are of special interest for applications.

The first of the latter cases to be reported appears to have been the tetrafluoroborate (BF_4^-) of a quaternary ammonium cation, which was discovered in 1984.[9] This salt (methoxyethyl dimethyl ethylammonium tetrafluoroborate, $MOENM_2E\text{-}BF_4$) melts at 13 °C and, on cooling, only loses its fluidity at a glass-transition temperature of $T_g = -98$ °C. However, although the authors of the report recognized their finding as "an important development in ambient-temperature molten-salt-supporting electrolytes", and reported three years later[10] a case (methoxymethyl dimethyl ethylammonium tetrafluoroborate, $MOMNM_2E\text{-}BF_4$) of even lower T_m (−16 °C) and T_g (−115 °C), they did not develop the subject nor report all their findings. For fundamental reasons,[9] these liquids did not support the decoupled Li^+ transport phenomenon that was in focus at Purdue University at that time. Indeed, there was no follow-up until Cooper and O'Sullivan[11] and Wilkes and co-workers,[12] in close succession in 1992, reported systematic studies of the fluorinated anion class of ionic liquids and set the stage for the current flowering of interest in this field.[13−22]

One of the reasons for the high fluidity of these liquids is the weak van der Waals interaction between the F atoms of the anions and their neighboring cations.[23] This is manifested in the low T_g values that are reported.[9,10,15,17] However, although the T_g value of the second Cooper ionic liquid ($MOMNM_2E\text{-}BF_4$)[10] remains the lowest on record, the fluidity at ambient temperature (which is now reported here for the first time) has been surpassed by several other formulations. Also, the ambient-temperature ionic conductivity of this salt, although five times higher than the 1.7 mS cm^{-1} value of the initial case[9] (in which the cation contained one extra CH_2 group), is also well below those of recently reported ionic liquids.[13−18] Clearly, there are other factors besides the starting point of the liquid state (T_g) involved in determining the ambient-temperature values of these important properties. The rates at which the fluidities of different formulations change with temperature must be very different, implying that there is much to understand about the dynamics of particle motion in this class of fluid.

Because one of the attractive features of the ionic liquid class of fluids is the extended temperature range of liquid-state behavior they offer, it is important to understand the effect of

* Author to whom correspondence should be addressed. E-mail: CAA@asu.edu.
[†] Arizona State University.
[‡] Purdue University.
[§] Now at IBM T. J. Watson Research Center, Yorktown Heights, NY.

10.1021/jp0275894 CCC: $25.00
Published on Web 05/31/2003

temperature on the various liquid properties. It is the purpose of the present paper to elucidate this problem and thereby bring the phenomenological description of ionic liquids in line with that which is common for other fluids. A point of interest in relation to fundamental understanding of liquids is that ionic liquids are single-component systems in which the cations and anions may possibly play independent roles in determining the liquid behavior.

In addition to data on salts containing familiar anions such as I^-, BF_4^-, triflate ($CF_3SO_3^-$), ClO_4^-, and bis-trifluoromethanesulfonyl imide ($TFSI^-$) anions, we will present some data for salts of large anions. These include the enlarged version of $TFSI^-$, bis(perfluoroethanesulfonyl) imide (known as $BETI^-$), and the new BOB^- anion (bis-oxalato-orthoborate),[24] whose behavior in nonaqueous solutions and Li^+ ion cells is currently proving to be of great interest.[25,26] More-detailed studies of the orthoborate anion class of ionic liquid will be reported subsequently.[27] Finally, some alternative tetrahalide anions, $FeCl_4^-$ and $GaCl_4^-$, have been included, because it was determined long ago[5] that the lowest glass temperatures of ILs were obtained with $FeCl_4^-$ anions.

Experimental Section

Materials. The chemicals used in this work were obtained from Aldrich, except for LiTFSI and LiBETI, which were received as gratis from 3M, and all were used as received.

Syntheses and Characterization. The synthetic procedures used for making the two Cooper quaternary ammonium tetrafluoroborate salts (i.e., $MOMNM_2E$-BF_4 and $MOENM_2E$-BF_4) were described in earlier reports[9] in which they were applied to prepare the iodide salts. The advantages of introducing ether groups into the side chains were also outlined in that work. The tetrafluoroborates characterized previously were obtained using $AgBF_4$ solutions in acetone to precipitate AgI from solutions of the iodides in acetone or acetonitrile, followed by removal of solvent by rotary evaporation and vacuum oven drying.

In the present work, the methoxyethyl dimethyl ethylammonium salts of tetrachlorogallate and tetrachloroferrate were prepared in a nitrogen-filled drybox by mixing stoichoimetric methoxyethyl dimethyl ethylammonium chloride and gallium(III) chloride or iron(III) chloride at room temperature.

The other quaternary ammonium salts and the 1-*n*-butyl-3-methyl imidazolium salts were produced by refluxing the onium chlorides with lithium or sodium salts of different anions in acetonitrile solutions. This inexpensive procedure, which will be described in more detail elsewhere,[27] yielded products without NMR-detectable Na^+ impurities when sodium salts were used in the preparation. No NMR resonances characteristic of residual water or solvents could be detected by NMR spectroscopy. The water-stable ionic liquids (both hydrophilic and hydrophobic) synthesized in this manner were checked for residual chloride using aqueous $AgNO_3$ solutions, and no AgCl precipitate could be detected in hydrophobic ionic liquids and hydrophilic ones that were prepared using sodium salt intermediates. When lithium salt intermediates were used, very weak Li NMR signals could be seen and traces of residual chloride were detected (with the exception of LiTFSI and $LiPF_6$, because of water washing in the procedure). However, these impurities in the ILs were insufficient to affect the measured physical properties.

Notation. In this paper, we will use the notation indicated at the start of the previous section for the quaternary ammonium salts of this study. However, we take note of an alternative notation that has some advantages, namely, $MOMNM_2E = N_{(1-O-1)112}$, $MOENM_2E = N_{(1-O-2)112}$, etc. This latter notation would be more consistent with previous usage[19,23] and is more adaptable to the cations with longer alkyl groups. It will be used in one of the summary diagrams, where economy of space becomes an issue. For imidazole-based cations, we will use B and M to denote the *n*-butyl and methyl side groups, respectively; thus, BMI^+ represents the 1-*n*-butyl-3-methyl imidazolium cation. For pyridine-based cations, we will use B to represent *n*-butyl-capping; thus, BPy^+ represents the *n*-butylpyridinium cation.

Glass-Transition Temperatures. The T_g values of most of the ionic liquids of this study were determined using a differential scanning calorimeter (model DSC-7, Perkin−Elmer) in the temperature range from −150 °C to 80 °C. The instrument temperature scale was calibrated at the crystal−crystal transition of cyclopentane (−151.16 °C) and the melting point of indium (+156.60 °C). Samples were sealed in aluminum pans and scanned at a rate of 20 K·min^{-1} in a helium atmosphere.

For the quaternary ammonium salts of $TFSI^-$, except for $MOENM_2E$-TFSI, the values of T_g were determined using a simple differential thermal analysis (DTA) instrument in the temperature range from −150 °C to 80 °C. The instrument was calibrated in an ice−water mixture ($T = 0$ °C), at the solid−solid transition temperature of anhydrous cyclohexane (99.5%, $T_{S1\rightarrow S2} = -86.6$ °C) and at the melting point of anhydrous ethylbenzene (99.8%, $T_m = -95.0$ °C). Samples were sealed in Pyrex glass tubes in a drybox filled with argon, quenched in liquid nitrogen, and then scanned during heating at ca. 20 K·min^{-1}. The T_g values reported are the onset values for upscans.

Conductivities. The conductivities of the ionic liquids were measured by the standard complex impedance method, using a Hewlett-Packard model HP 4192A LF impedance analyzer in the frequency range from 5 Hz to 1 MHz. We used sealed dip-type cells containing two parallel platinum disks. The cell constants were 0.5−0.7, calibrated with a 0.1 m KCl aqueous solution to a precision of 0.2%. Measurements were made during controlled slow cooling from 120 °C to −50 °C. The cooling rate was low enough that the data points differed negligibly from those obtained in static isothermal measurements.

Viscosities. The dynamic viscosities of the quaternary ammonium salts of BF_4^-, $GaCl_4^-$, and I^- were obtained using a Wells−Brookfield cone−plate digital viscometer, which has the advantage that only small samples are required and the disadvantage that it is not a high-precision device. The optimum volume of 1.0 mL was determined using *o*-terphenyl as the calibrating fluid, and values that agreed with the literature data to better than 5% at high temperatures (considerably better at $T < 100$ °C) were obtained using a model CP-40 conic spindle (Wells−Brookfield).

The kinematical viscosities of other ionic liquids were measured between ambient temperature and 150 °C, using Cannon−Ubbelohde viscometers. $CaCl_2$ drying tubes were used to protect the samples from moisture in the air. The viscometers were placed within a tall, aluminum, temperature-smoothing block, and the temperature of the sample was maintained for half an hour before measurement. The precision of measurement with Cannon−Ubbelohde viscometers is controlled by the reproducibility of flow times, and the accuracy is controlled by the accuracy of the calibration constants and by the temperature measurement. Precision was limited at the highest temperatures (at >100 °C) by the short flow times (<10 s), which were a consequence of our use of a single viscometer for each sample. The flow times were reproducible: the standard deviation was ±0.2 s. For temperatures <40 °C, the run times are typically

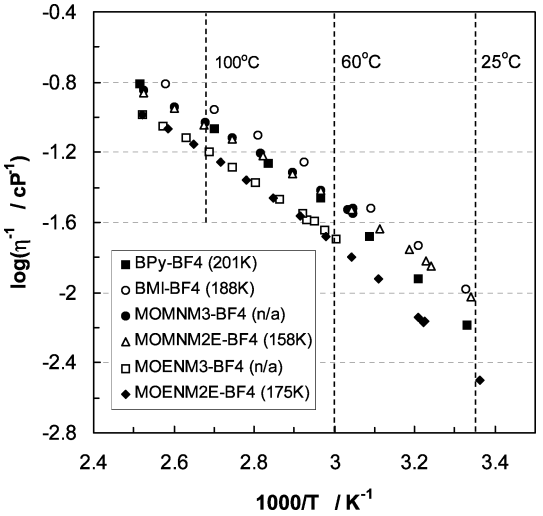

Figure 1. Arrhenius plots of fluidities of tetrafluoroborate (BF_4^-) ionic liquids of various quaternary ammonium cations, compared with data for aromatic cations with the same anion. The glass temperatures, in degrees kelvin, are indicated in parentheses.

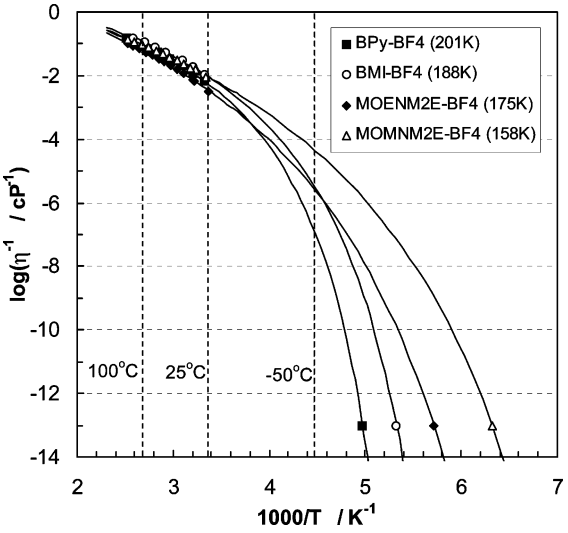

Figure 2. Data of Figure 1 plotted on an expanded scale to include values at the glass-transition temperature. Note the crossovers of aromatic and nonaromatic systems. The glass temperatures, in degrees kelvin, are indicated in parentheses.

200 s or longer; hence, the reading error is only 0.1% of the efflux time.

Densities. In this work, densities were measured by simple and not very precise means, only to compare the behavior of the different systems on a Walden plot, which demands the use of equivalent conductivities, $\Lambda = \sigma V_E$, where σ is the specific conductivity and V_E is the volume containing one Faraday of positive charge.

The density values at different temperatures were obtained with accuracy of ~1% by measuring the weight of the sample in a 2.00 mL volumetric flask held in a drybox. The flasks were held in an aluminum heating block at the measured temperature for half an hour to obtain a uniform temperature before measurement.

Results

Data for fluidities (η^{-1}, where η is the viscosity measured in centipoise (cP); 1000 cP = 1 Pa s) of tetrafluoroborate ionic liquids, the majority of which date from ca. 1984,[28] are shown in Figure 1, in the common Arrhenius form.

In Figure 2, we replot the data of Figure 1, including the value of fluidity at its onset point (namely, the glass-transition temperature, T_g) as a data point for each salt. This fluidity value is not the inverse of the classical 10^{13} P at T_g of silicate glass science.[29] Rather, it is the inverse of the smaller value ($\eta(T_g) \approx 10^{11}$ P) that has been found more typical of liquids that have T_g values below room temperature.[30] Two specific cases are of special relevance to the present work, because of their study over wide viscosity ranges, which permit short extrapolations to the values at T_g. These are the studies by Moynihan and coworkers[31] of ionic liquids of the molten hydrate and ultraconcentrated aqueous solution type, e.g., $Ca(NO_3)_2 \cdot 4H_2O$ and $Ca(NO_3)_2 \cdot 8H_2O$. This value appears to be generally applicable to liquids whose glass temperatures fall in the range of the present systems. This is mainly because (i) it is the enthalpy relaxation time (τ), not the viscosity, that remains constant at T_g,[29] and (ii) the shear and enthalpy relaxation times are very similar. The viscosity at T_g depends on the value of the shear modulus G_∞, through the Maxwell relation $\eta = G_\infty \tau$, and G_∞ generally scales with T_g.[29,31] Note that we have plotted our fluidities using units of inverse centipoise (cP^{-1}), so our fluidity value at the calorimetric T_g is 10^{-13} cP^{-1}.

Inclusion of the fluidity at T_g permits us to plot out the course of the fluidity over the entire liquid range for the different liquids of this study. This has the great advantage of making clear why the BF_4^- salts of quaternary ammonium cation salts are not the most fluid at room temperature, despite their lower T_g values. The reason is that the liquid property known as "fragility" (which refers to the rate at which the transport properties change with temperature near the glass transition) is small for salts of these cations, relative to the values for the salts with aromatic cations. This will be discussed further in the next section.

Note that the lines passing through the data points in Figure 2 are not "guides to the eye" but, rather, are plots of the best-fit Vogel−Fulcher−Tammann (VFT) equations for fluidity ϕ,[29]

$$\phi = \phi_0 \exp\left(\frac{B}{T - T_0}\right) = \phi_0 \exp\left(\frac{DT_0}{T - T_0}\right) \qquad (1)$$

where ϕ_0, B, D, and T_0 are constants and D is inversely proportional to the fragility of the liquid.

In Figures 3 and 4, we examine the effect of changing the anion while keeping the cation constant. We do this for one example of each class of cation: aromatic (BMI^+) in Figure 3 and nonaromatic (the substituted ammonium cation, $MOENM_2E^+$) in Figure 4. Note that, consistent with the findings of ref 5, the lowest glass temperature—and, here, also the highest fluidity—is obtained with the tetrachloroferrate ($FeCl_4^-$) anion.

In Figure 5, we present a collection of conductivity data for various salts (including data from earlier unpublished work[28]), which will be used in conductance/fluidity correlations to be discussed in the next section. We note the existence of liquids with conductivity as high as 10^{-5} S cm^{-1} at −50 °C.

Discussion

As noted earlier in Figure 2, there is a crossover in the fluidity of the tetrafluoroborates of the quaternary ammonium cation methoxyethyl dimethyl ethylammonium, and dialkyl imidazolium cations, at approximately −70 °C, a temperature below which the quaternary ammonium salts would become the most fluid. To help understand the reasons for this phenomenon, we turn to the T_g-scaled Arrhenius plot (Figure 6), a means by which the viscosity data on a great variety of liquid types can be

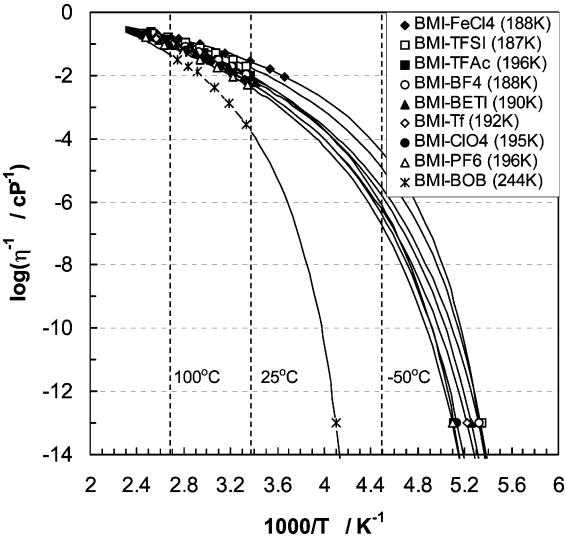

Figure 3. Arrhenius plots of the fluidities of salts combining the 1-*n*-butyl-3-methylimidazolium (BMI^+) cation with various anions. The glass temperatures, in degrees kelvin, are indicated in parentheses.

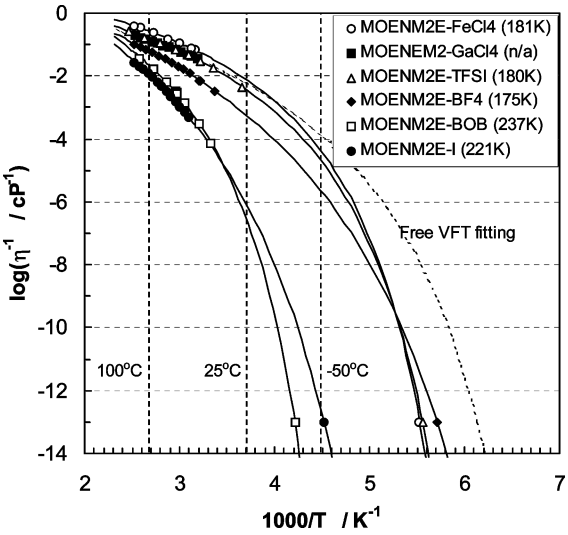

Figure 4. Arrhenius plots of the fluidities of salts combining the quaternary ammonium salt methoxyethyl dimethyl ethylammonium ($MOENM_2E^+$) cation with various anions. The glass temperatures, in degrees kelvin, are indicated in parentheses.

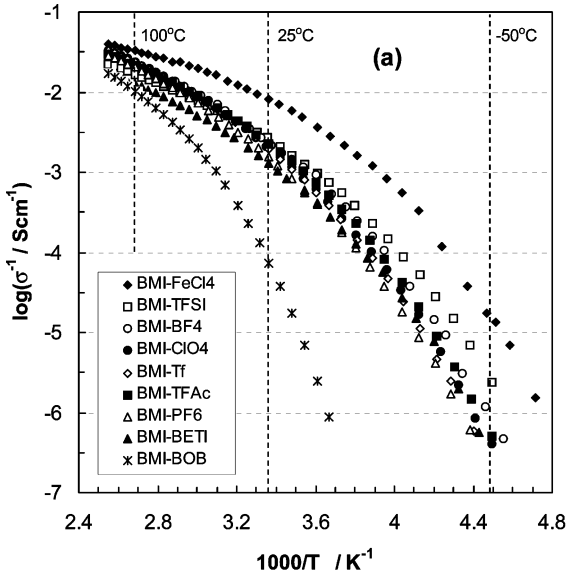

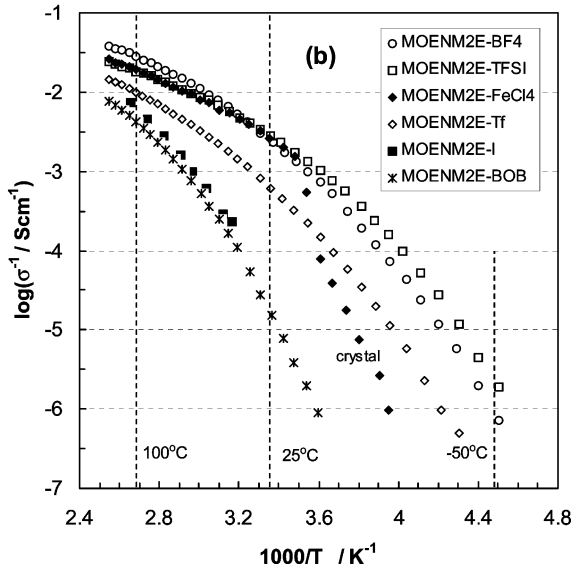

Figure 5. (a) Arrhenius plots of ionic conductivity of BMI^+ cation combined with various anions. (b) Analogue of panel a for the quaternary ammonium cation of Figure 4. Some conductivities (e.g., of $FeCl_4^-$ and BOB^- salts) are low, relative to those of the aromatic cation BMI^+ cases. The rapid decrease of (apparent) conductivity with temperatures below 15 °C for the case of $FeCl_4^-$ anion is due to crystallization effects.

brought together for comparison. This T_g-scaled presentation of viscosity data was first used by Oldekop[32] for liquid silicates, and later by Laughlin and Uhlmann[33] to compare certain molecular liquids with liquid silicates. It has recently been much used by our group[34] in an ongoing attempt to understand the general problem of the physics of liquid excitation. Now, we take the data for the two salts in question, along with additional cases from Figures 3 and 4, and place them on Figure 6 (see large open symbols for the new ionic liquid data).

We should note that these are not the first organic salts to be included in this plot. Data for a chlorozincate of the pyridinium cation, which has a T_g value of 275 K, and also for α-methylpyridinium chloride, which has a T_g value of 225 K, were included in the original plot.[34b] Liquids that fall on the right-hand side of the plot are classified as "fragile", and the reason for their extreme temperature dependence near T_g is currently regarded as a challenging problem in condensed-matter physics. We note that the most fragile of the ionic liquids of Figures 2−4, BMI−BOB, is close to the fragility edge defined by the molten nitrates (among the ionic systems) and by some newly characterized organic liquids Decalin and decahydroisoquinoline[36−38] (among molecular liquids). It is possible that replacing the butyl group with a shorter alkyl group may lead to even more-fragile systems.

By contrast, the quaternary ammonium tetrafluoroborates are found almost in the middle of the diagram, where, previously, only small molecule paraffins and liquids with some source of intermediate range order, were found. Figure 6 shows the overlap of data for one of the present cases, $MOENM_2E^+BF_4^-$, with data for the hydrogen-bonded liquid, propanol, $ZnCl_2$, and anorthite ($CaAl_2SiO_8$, T_g = 1134 K). The latter is a highly distorted aluminosilicate network and the former two both have associated character, through hydrogen bonding and chloride bridge bonding, respectively.

A plot of this type, incorporating a variety of tetrasubstituted ammonium cations, was shown with the 1983 ionic liquid data in ref 9. It showed essentially the same (intermediate) behavior,

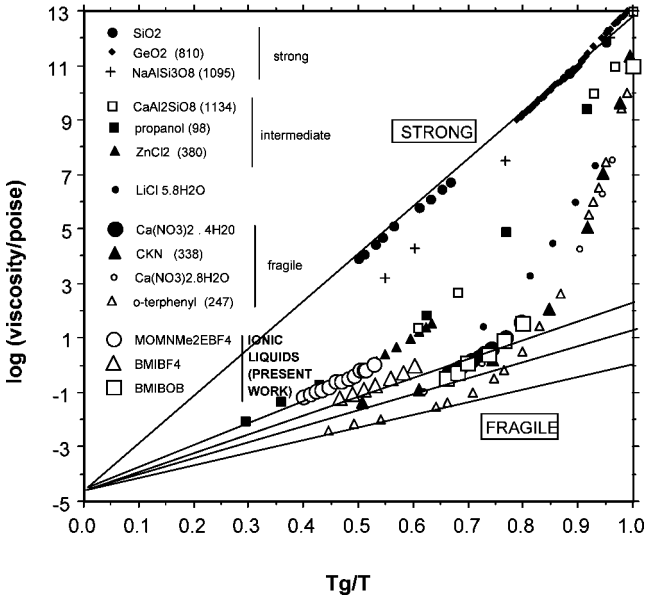

Figure 6. T_g-scaled Arrhenius plots of viscosities of three of the ionic liquids from the present work (large open symbols), compared with more-extensive data sets for liquids of other types. The glass temperatures, in degrees kelvin, are indicated in parentheses. Note the spread of ionic liquid character, from intermediate to extremely fragile.

for the ionic conductivity, of all the quaternary ammonium ILs of the study, including their solutions with lithium iodide (LiI) up to very high LiI contents. This behavior marks them as interesting academically, because the intermediate liquids in Figure 6 tend to show the simplest behavior[34] and, hence, offer the best opportunities for straightforward theoretical interpretation. For instance, viscosity data over some 13 orders of magnitude of such liquids can be well described using a single parameter set in the three-parameter VFT equation (eq 1). However, for performance as high-fluidity ambient-temperature liquids, the intermediate behavior in Figure 6 is a serious disadvantage.

It is possible that combination with the correct type of anion could modify this behavior in the favorable direction of increased fragility; however, such an anion has not been revealed in the present work. Even the combination with the BOB^- anion, which gives such high fragility with aromatic cations, only gives rise to a small increase in fragility, although there is a large increase in the glass temperature (see Figure 4). The important role played by aromaticity in promoting fragility reminds us of the similar pattern shown by molecular liquids some time ago.[35] In ref 35, molecules such as toluene were observed to be very fragile while their paraffinic analogues (e.g., methyl cyclohexane) were intermediate. No explanation of this distinction has been provided, although it would seem that it cannot lie just in the presence of π-clouds on the aromatic rings, because the most-fragile liquids identified to date are nonaromatic (Decalin and decahydroisoquinoline[36−38]).

Keeping the anion constant (BF_4^-), we can see, from Figure 7a, that the *n*-butylpyridinium cation (BPy^+) provides the greatest fragility. The effect on anions of different character can be seen from Figure 7b, using the case of the cation (BMI^+) being kept common. It is seen that there is little anion effect, except for the case of the BOB^- anion, which apparently induces high fragility. It is natural to ask if the cation and anion effects can be combined, and, indeed, it is found that the salt BPy−BOB, not shown in Figures 6 and 7, has a slightly higher fragility than BMI−BOB (ref 27). The latter case indeed overlaps the canonical fragile melt CKN [$40Ca(NO)_3)_2 \cdot 60KNO_3$] almost exactly in Figure 6. Thus, ionic liquids, despite having much lower glass temperatures than the mixed nitrate melts, overlap them in fragility.

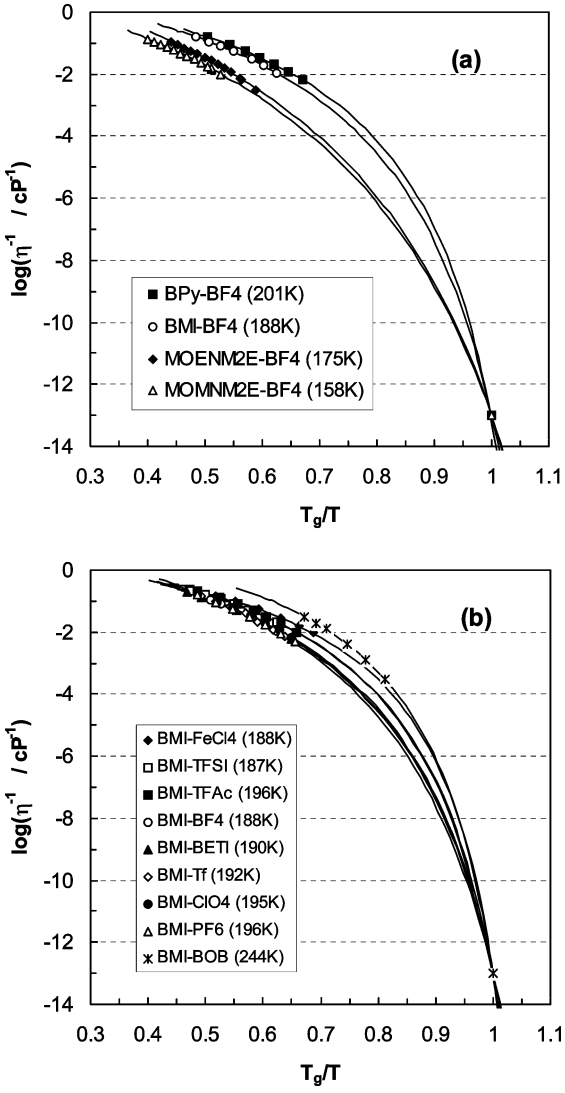

Figure 7. (a) T_g-scaled Arrhenius plot of fluidities of (a) tetrafluoroborates of different types of cations. (b) Salts of BMI^+ with various anions. Note the distinction of BOB^- salt in panel b.

Among the ionic liquids of this study, it is generally found that the most-fragile cases are also the cases with the highest T_g values. However, the idea that the higher fragility might be caused merely by the higher T_g value seems to be eliminated, not only by the previously mentioned comparison with CKN, but also by comparison with the present case of the iodide of $MOENM_2E^+$ (seen in Figure 4). This quaternary ammonium iodide has a very high T_g value but one of the lower fragilities. Statistically, it is more likely that high fragility will be found among salts of higher T_g values, simply because there are more of them.

What actually controls the fragility in these systems, unfortunately, is not made any clearer by these observations. On the other hand, the study does provide some excellent single-component systems for use in follow-up studies, such as the neutron scattering density of vibrational-state determinations, which will be more diagnostic for fragility origins. Irrespective of origins, it is impressive to see, in Figure 3, how the high fragility of BMI−BOB compensates for the effect of high T_g values, so as to provide a common value for the fluidity at ~150 °C.

The Walden Plot in Relation to Ionic Liquid Properties. So far, we have not discussed the relationship between conductivity and viscosity. Elsewhere,[39−41] we have discussed the merits of the Walden plot for organizing the different possible relations between the conductivity per mole of charge (i.e., the equivalent conductivity Λ) and the fluidity $\phi = \eta^{-1}$ (where η is the viscosity). This scheme is particularly apt for the case of ionic liquids, because it provides the basis for understanding the relationship between conductivity and low vapor pressure that is, otherwise, not so obvious. It is based on Walden's original observation[42] for the case of aqueous solutions of strong electrolytes, that the equivalent conductivity, $\Lambda = \sigma V_E$ (where V_E is the volume containing one Faraday of positive charge), of strong electrolytes is large, in inverse proportion to the magnitude of the viscosity, and that it changes with temperature at the same rate as the inverse viscosity. This is summarized in the Walden Rule,

$$\Lambda\eta = \text{constant} \tag{2}$$

The Walden rule is interpreted in the same manner as the Stokes−Einstein relation[43] for the relation between the self-diffusivity D of species i, in a medium of viscosity η, and its radius r_i:

$$D_i = \frac{k_B T}{6\pi\eta r_i} \tag{3}$$

In each case, it is supposed that the frictional force impeding the motion of ions is a viscous force that is due to the solvent through which the ions move. It is most appropriate for the case of large ions moving in a solvent of small molecules. However, we will see here that, just as the Stokes−Einstein equation applies well to pure liquids,[43] the Walden rule also applies, rather well, to pure ionic liquids. When the units for fluidity are chosen to be reciprocal poise (P^{-1}) and those for equivalent conductivity are $S{\cdot}cm^2{\cdot}mol^{-1}$, this plot has the particularly simple form shown in Figure 8. Figure 8 contains data for many of the salts of the present study. It includes data for systems with fluidities that vary by more than 8 orders of magnitude. To fix the position of the "ideal" Walden line, we include some data for dilute aqueous KCl solutions in which the system is known to be fully dissociated and to have ions of equal mobility. For the unit chosen, the ideal line runs from corner to corner of a square diagram. We comment on the present data after noting some features of the plot that are not normally discussed.

First, we note that, for ionic liquids, the most favorable systems will have their ambient-temperature values located in the top right-hand corner of the diagram. These will be the systems in which high fluidities are combined with high conductivities. For applications such as solvent media for "green" synthetic reactions,[16,20] the importance of having high conductivities is not obvious until one considers the relationship between high conductivity and the property of practical importance—the low vapor pressure. Both latter properties are dependent on the formation of an "ideal" quasi-lattice. In the ideal quasi-lattice, there is a uniform, although nonperiodic, distribution of positive charge around negative charge, such that the system acquires a Madelung energy (E_{Mad}) that is comparable to that of the ideal ionic crystal. In such a quasi-lattice, ionic motions are not correlated in ways that lead to diminished conductivity; i.e., no ion pairs exist, at least not for any statistically significant periods of time.[44−47]

The more ideal the quasi-lattice formed, the larger the Madelung energy of the liquid, hence the larger the energy that must be provided to extract an ion pair into the vapor state. The latter quantity determines the vapor pressure at any temperature T, via the Boltzmann factor ($\exp[\Delta h_{vap}/(RT)] \approx \exp[E_{Mad}/(RT)]$). Thus, ionic liquids that have their "Walden points" on the ideal line will have the lowest vapor pressures.

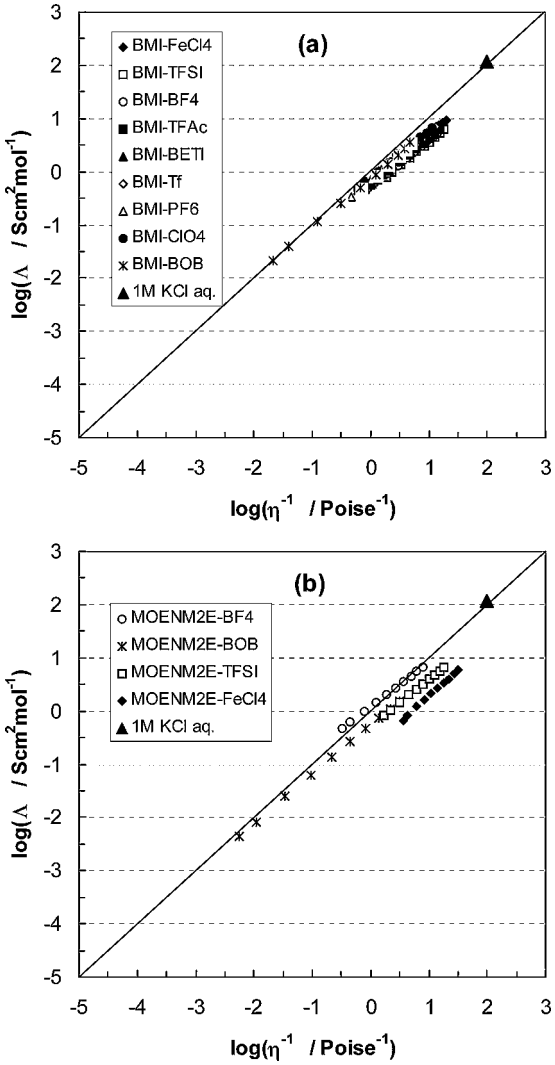

Figure 8. Walden plot for different salts with BMI^+ cations, showing almost-ideal behavior for BOB salt. The data for a dilute aqueous KCl solution are included to fix the position of the "ideal" Walden line.

Poor Ionic Liquids, and the Walden Plot as a Classification Diagram. Not all ionic liquids behave as ideally as those shown in Figure 8, on the basis of the salts of the BMI^+ cation. Figure 9 shows a group that is based on the substituted ammonium cations. One of the tetrafluoroborates, that which contains the cation $MOMNM_2E^+$, is seen to have a conductivity that is almost an order of magnitude less than ideal. Such a liquid must have a high degree of correlation in the motion of its cations and anions to explain the poor conductivity at a given fluidity, and would also be expected to have a much higher vapor pressure than the salts with ideal Walden behavior.

The trend for the latter salt in Figure 9 is the same as that seen previously in nonaqueous electrolyte solutions in which spectroscopic studies have shown that ion pairing is prevalent.[48] It is certainly not obvious why there should be any tendency toward ion pairing in this liquid, when closely related cases, differing by only one C atom, behave ideally. It is possible that there are particular interionic "recognition" effects, conceivably involving ion triplets, which are responsible for the unexpected behavior. Such effects could derive from electron depletion of

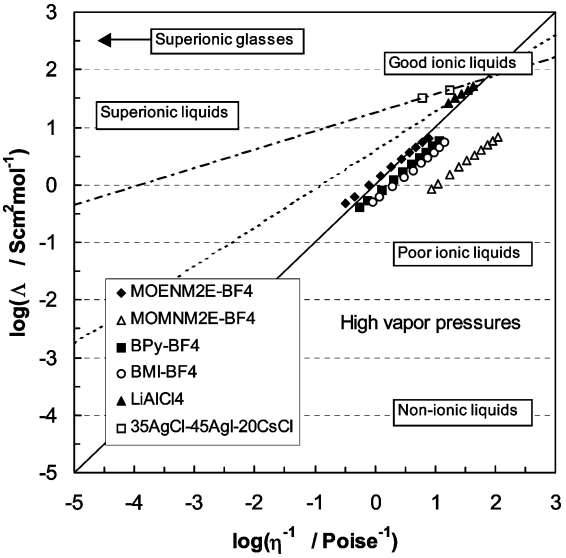

Figure 9. Walden plot for tetrafluoroborate salts of various cations, showing associated (or "supercoupled") behavior of the salt of the cation $MOMNM_2E^+$. By contrast, the salt of $MOENM_2E^+$ may become decoupled at low temperature. The dotted lines passing through the $LiAlCl_4$ points and the AgCl−AgI−CsCl points are the fits of eq 4 to the data points. The slope, α, is inversely proportional to the logarithm of the decoupling index, R_τ, of ref 51. The plot is annotated to indicate how it may serve as a classification diagram for ionic liquids and other electrolytes.[41]

the methylene group positioned between the O^{2-} and N^+ ions, making the methylene protons acidic enough to form significant hydrogen bonds to the fluorinated anions. Whatever the explanation may be, Figure 9 shows that ideal behavior cannot be taken for granted in these systems.

It is interesting that this salt with the low Walden product is also the case in which the glass temperature has the lowest value of this study. The decreased E_{Mad} value implied by the small Walden product may be a part of the reason. The same correlation of low glass temperature with a large ion-pairing propensity was seen earlier with solutions of lithium triflate in polyether solvents.[48] Provided that the effect is not large enough to raise the vapor pressure to unacceptable values, such limited ion-pairing effects could have a favorable effect on the fluidity, by lowering the glass temperature. A careful study of the vapor pressure, in relation to Walden rule deviations, would make an interesting study for this reason, as well as for the fundamental interest content of the question.

The fundamental reason why liquids in which ion pairing occurs should have vapor pressures higher than the ideal is the reduced electrical work needed to remove an ion pair into the vapor phase. We can therefore use the lower right-hand half of the diagram to represent "poor" ionic liquids. In the limit, the properties of a poor ionic liquid will approach the behavior of molecular liquids.[40] There should be a series development of this molecular liquid behavior, as proton-transfer acids and bases of increasingly similar pK_a values (e.g., imidazole (pK_a = 6.99) and acetic acid (pK_a = 4.75)) are combined. Results of such studies will be reported elsewhere.[49]

By contrast, the top left-hand corner of the diagram can be used to represent superionic liquid and glass behavior, because the latter combine high conductivities with *low* fluidities. Except at high temperatures, such systems cannot be of much use as high fluidity systems, although they may be of great interest as single-ion conductors for battery electrolyte purposes. We can anticipate the behavior of such systems by making use of the values of conductivity, density, and viscosity for $LiAlCl_4$ available in Janz[50] (extrapolated to pure $LiAlCl_4$ from binary solution data where necessary), and the corresponding data for the AgCl−AgI−CsCl system from Angell and co-workers.[51a,b] Knowing the viscosity at T_g, and making use of the fractional Walden rule (which has been recognized since the early days of molten salt chemistry[52]), we can construct the dashed line seen in Figure 9. It is a straight line in the log−log plot, because the fractional Walden rule is written as

$$\Lambda\eta^{\alpha} = \text{constant} \tag{4}$$

where α is a constant between zero and unity. In the log−log plot of Figure 9, the slope of the Walden line is given as α. The exponent α, which is inversely proportional to the logarithm of the "decoupling index", is used to describe the decoupling of mobile ion relaxation modes from matrix modes in superionic conductors.[51]

The decoupling index is used to characterize the quality of superionic materials under consideration for solid-state electrochemical device applications. It is not clear if this property will be developed much in ionic liquids, although MacFarlane and co-workers[53] have observed such behavior in the crystalline state of imidazolium halide salts. Certainly, superionic systems will not be found in any dilute solutions of lithium salts in ionic liquids, because of the counter polarization effects described in ref 9. These conspire to form Li^+ ion traps, which are weak in the case of unpolarizable ions but never absent.[9] Thus, the energy barriers opposing Li^+ ion motion can never be smaller than those for viscous flow; i.e., the value of α in eq 4 is ≥1. The parameter α was originally interpreted as the ratio of activation energies for conductance and viscous flow. For systems that do not obey the Arrhenius law, α represents the ratio of *B* parameters in eq 1 for the two processes. The physical meaning of *B* can be very different in different theoretical interpretations of eq 1.[54]

It might be noted, before leaving Figure 9, that the increase in ion pairing commonly observed with increasing temperature affects the slope of the Walden plot in the same sense as the presence of ion decoupling. The two effects can be distinguished by the side of the ideal Walden line on which they cause the data to fall. Thus, the departure from ideal Walden behavior, which is seen in the case of most ionic liquids at high temperature (see Figure 8), is, most likely, the result of the onset of some sort of correlation in cation and anion positions. This can best be thought of as manifestation of the interactions that would eventually result in vaporization if decomposition were not to occur first.

Optimization of Ionic Liquid Performance: The Glass-Transition Temperature and the Pair Potential. We previously noted that both the T_g value and the fragility are involved in determining the fluidity of a given salt at ambient temperature. Although the factors that determine the fragility remain very unclear, there seems some hope of rationalizing the value of the glass temperature. This should be determined by the cohesive energy, which, for the unassociated salts that fall on the ideal Walden plot, relates to the depth of the potential energy minimum for pairs of oppositely charged ions in the bulk liquid. The position and depth of this minimum is determined by the balance of attractive and repulsive contributions to the cation−anion pair potential. The repulsive forces are understood in terms of Pauli repulsions, as closed electron shells on the outer parts of the oppositely charged ions try to overlap. The attractive forces come from the gradient of some combination of the coulomb cohesive energy, which decreases with the sum of the effective ionic radii, and the van der Waals energy that must

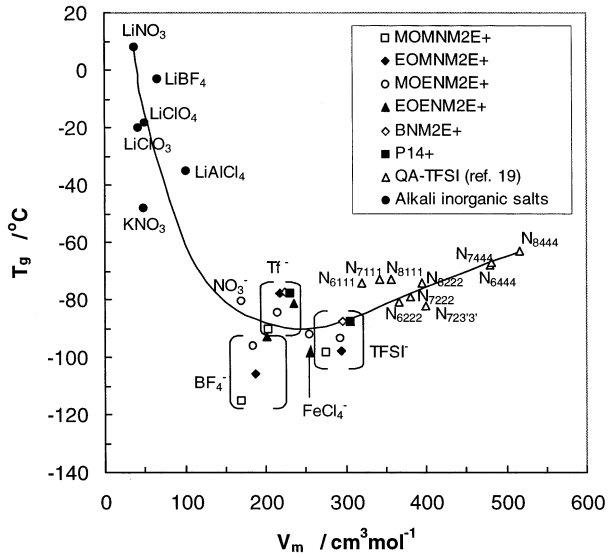

Figure 10. Dependence of the cohesion of salts of weakly polarizable cations and anions, assessed by the T_g value, on the ambient-temperature molar volume, V_m, and, hence, on the interionic spacing [$(r^+ + r^-) \approx V_m^{1/3}$]. A broad minimum in the ionic liquid cohesive energy is seen at a molar volume of 250 cm^3 mol^{-1}, which corresponds to an interionic separation of ~0.6 nm, assuming a face-centered cubic packing of anions about the cations. The lowest T_g value in the plot should probably be excluded from consideration, because of the nonideal Walden behavior for this IL ($MOMNM_2E^+BF_4^-$) (see Figure 9). For the data from ref 19 on imides of large tetraalkylammonium cations, the compact nomenclature of that paper has been retained for easy identification of cations. Data for inorganic nitrates are from refs 55 and 60; for $LiBF_4$, $LiClO_4$, and $LiClO_2$, from ref 60; and for $LiAlCl_4$, from ref 51b. The line through the points is a guide to the eye.

increase with increasing ionic size (although at different rates for polarizable and nonpolarizable ions). Thus, a minimum should exist in the relationship between T_g and the radius sum, the position of which has not, to date, been discussed in the literature.

The minimum in the plot of T_g versus interionic separation should occur at a smaller radius sum for polarizable species than for nonpolarizable species. As discussed elsewhere,[23] the coulomb energy should vary as the inverse first power of the internuclear separation, whereas the van der Waals interaction should be determined more locally through the interaction of the outer shell atoms. Therefore, salts of singly charged ions containing large anions with fluorinated components on the exterior should maintain lower T_g values at large molar volumes than those of salts with nonfluorinated anions, such as BOB^-.

Although it is difficult to assess the effective ionic radii from structural formulas, the effective *sums* of the radii are well represented by the cube roots of the molar volumes. Strictly, the molar volume used for this purpose should be measured at the T_g, whereas the relevant density data are usually only available near the ambient temperature. However, the effect of temperature on the volume between the ambient temperature and the typical T_g is always very small (<2%), relative to the range of volumes that are covered by the salts of this study. Therefore, we adopt the molar volumes at ambient temperature as a basis for judging the combinations of anions and cations that might lead to a minimum values of T_g. Clearly, identification of such combinations would provide a useful guide to likely "good" ionic liquids, provided that the melting points and fragility factors were also favorable.

In Figure 10, T_g is plotted versus the molar volume (V_m) for all the salts of quaternary ammonium cations with fluorinated anions, and with oxyanions in which the oxygen charge is strongly polarized toward the molecule ion center (e.g., ClO_4^-, FSO_3^- (no data), $CF_3SO_3^-$, and NO_3^-), for which the van der Waals interactions should not be too important. Salts with aromatic cations were excluded, because of the greater polarizability originating in their π-electron clouds. We include, at small volumes, some points obtained by short extrapolations of binary solution data,[55] for nitrates and perchlorates of potassium and lithium cations, to form some idea of the behavior of the T_g-vs-V_m relation at small volumes. To continue this steep part of the curve, we include data for $LiAlCl_4$[51] and the nitrate of $MOENM_2E^+$.[57] For other quaternary ammonium salts, we use data for the $TFSI^-$ anions, both from the present study and from the study of Sun et al.[19] The latter authors studied salts with molar volumes up to 500 cm^3 and their T_g values are clearly on the van der Waals interaction-dominated side of the minimum.

It appears from Figure 10 that the anticipated minimum in T_g occurs at $V_{m(min)} \approx 250$ cm^3 mol^{-1}, corresponding to a cation−anion separation of centers of ~0.6 nm, if we consider the simplest possible packing (face-centered cubic for a given ion type, simple cubic for all ions, such as the NaCl structure). Clearly, there is a great deal of scatter in the T_g-vs-V_m relation, so there must be important specific factors to be taken into account. We have identified only the background trend.

Data for large unfluorinated anions are not available, except for the case of BOB^- from the present work. If the data for BOB^- salts are any indication, the minimum in the T_g-vs-V_m relation will be narrower for the case of polarizable anions, because polarizable thiocyanate and dicyanamide anion salts have low T_g values.[58] The low T_g value, −104 °C, reported by MacFarlane et al.[58] for the salt 1-ethyl-3-methylimidazolium dicyanamide (which should be polarizable) should provide a point on the plot that would fall near its minimum. Comparisons with salts of the SCN^-, $C(CN)_3^-$, and $B(CN)_4^-$ anions would be desirable to test this speculation.

Concluding Remarks

By studying the relative properties of a variety of ionic liquid types, we have arrived at a broad picture of the physical behavior of these systems. Not studied yet are the properties of mixtures of these liquids, which, as shown from previous observations of the behavior of their molten hydrate equivalents,[59] can have wide ranges of immiscibility. The development of criteria for predicting immiscibility ranges in ionic liquids, which could be of value for separation sciences, will be the subject of future articles.

Acknowledgment. This work was supported, in its initial phase (1983−1986), by a grant from the Department of Energy and, in its current phase, by the National Science Foundation, Solid State Chemistry program, under Grant No. DMR 0082535. We are grateful to Dr. Li-Min Wang for helping measure the glass transition temperatures using the DSC-7 instrument. We are also grateful to Dr. Akitoshi Hayashi for some data analysis on decoupled ionic electrolytes, which contributed to the classification diagram (Figure 9).

References and Notes

(1) Walden, P. *Bull. Acad. Imper. Sci. (St. Petersburg)* **1914**, 1800.
(2) (a) Ford, W. T.; Hauri, R. J.; Hart, D. J. *J. Org. Chem.* **1973**, *38*, 3916. (b) Ford, W. T.; Hart, D. J. *J. Phys. Chem.* **1976**, *80*, 1001.
(3) Gordon, J. E.; Subbarao, G. N. *J. Am. Chem. Soc.* **1978**, *100*, 7445.
(4) Hurley, F. H.; Weir, T. P. *J. Electrochem. Soc.* **1951**, *98*, 203.

(5) Angell, C. A.; Hodge, I. M.; Cheeseman, P. A. In *Molten Salts, Proceedings of the International Conference on Molten Salts*; Pemsler, J. P., Ed.; The Electrochemical Society: Pennington, NJ, 1976; p 138.

(6) Wilkes, J. S.; Levisky, J. A.; Wilson, R. A.; Hussey, C. L. *Inorg. Chem.* **1982**, *21*, 1263.

(7) Hussey, C. L. *Adv. Molten Salt Chem.* **1983**, *5*, 185.

(8) Matsunaga, M.; Inoue, Y.; Morimitsu, M.; Hosokawa, K. *Proc.—Electrochem. Soc.* **1993**, *93*, 507.

(9) Cooper, E. I.; Angell, C. A. *Solid State Ionics* **1983**, *9&10*, 617. (See, in particular, the note added in proof.)

(10) Cooper, E. I.; Angell, C. A. *Solid State Ionics* **1986**, *18&19*, 570.

(11) Cooper, E. I.; O'Sullivan, E. J. *Proc.—Electrochem. Soc*. **1992**, *92-16*, 386. (*Proceedings of the 8th International Symposium on Molten Salts*; The Electrochemical Society: Pennington, NJ, 1992.)

(12) (a) Wilkes, J. S.; Zaworotko, M. J. *J. Chem. Soc., Chem. Commun.* **1992**, 965. (b) Carlin, R. T.; Wilkes, J. S. In *Chemistry of Nonaqueous Solutions*; Mamantov, G., Popov, A. I., Eds.; VCH Publishers: New York, 1994; Chapter 5. (c) Carlin, R. T. In *Molten Salts*; Gaune-Escarde, M., Ed.; NATO-ASI, Kluwer Scientific: Delft, The Netherlands, 2001.

(13) Bonhôte, P.; Dias, A.-P.; Armand, M.; Papageorgiou, N.; Kalyanasundaram, K.; Graetzel, M. *Inorg. Chem.* **1996**, *35*, 1168.

(14) McEwan, A. B.; Ngo, H. L.; LeCompte, K.; Goldman, S. L. *J. Electrochem. Soc.* **1999**, *146*, 1687.

(15) Sun, J.; Forsyth, M.; MacFarlane, D. R. *Ionics* **1997**, *3*, 356.

(16) (a) Bowles, C. J.; Bruce, D. W.; Seddon, K. R. *Chem. Commun.* **1996**, 1625. (b) Holbrey, J. D.; Seddon, K. R. *J. Chem. Soc., Dalton Trans.* **1999**, 2133.

(17) Hirao, M.; Sugimoto, H.; Ohno, H. *J. Electrochem. Soc.* **2000**, *147*, 4168.

(18) Matsumoto, H.; Yanagida, M.; Tanimoto, K.; Nomura, M.; Kitagawa, Y.; Miyazaki, Y. *Chem. Lett.* **2000**, 922.

(19) Sun, J.; Forsyth, M.; MacFarlane, D. R. *J. Phys. Chem.* **1998**, *102*, 8858.

(20) Welton, T. *Chem. Rev.* **1999**, *99*, 2071.

(21) Yoshizawa, M.; Ogihara, W.; Ohno, H. *Electrochem. Solid-State Lett.* **2001**, *4*, E25.

(22) Stuff, J. R.; Lander, S. W., Jr.; Rovang, J. W.; Wilkes, J. S. *J. Electrochem. Soc.* **1990**, *137*, 1492.

(23) Angell, C. A. In *Molten Salts: From Fundamentals to Applications*; Gaune-Escarde, M., Ed.; NATO-ASI, Kluwer Scientific: Delft, The Netherlands, 2001.

(24) Xu, W.; Angell, C. A. *Electrochem. Solid-State Lett.* **2001**, *4*, E1.

(25) Xu, K.; Zhang, S.-S.; Jow, T. R.; Xu, W.; Angell, C. A. *Electrochem. Solid-State Lett.* **2002**, *5*, A26.

(26) Xu, K.; Zhang, S.-S.; Poese, B. A.; Jow, T. R. *Electrochem. Solid-State Lett.* **2002**, *5*, A259.

(27) Xu, W.; Wang, L.-M.; Nieman, R. A.; Angell, C. A., submitted to *J. Phys. Chem.*

(28) Cooper, E. I.; Angell, C. A., unpublished work, 1986.

(29) Angell, C. A. *Pergammon Encyclopedia of Materials: Science and Technology*, 2001; Vol. 4, p 3365.

(30) Moynihan, C. T.; Macedo, P. B.; Montrose, C. J.; Gupta, P. K.; DeBolt, M. A.; Dill, J. F.; Dom, B. E.; Drake, P. W.; Easteal, A. J.; Elterman, P. B.; Moeller, R. P.; Sasabe, H. A.; Wilder, J. A. *Ann. N. Y. Acad. Sci.* **1976**, *279*, 15.

(31) (a) Ambrus, J. H.; Moynihan, C. T.; Macedo, P. B. *J. Phys. Chem.* **1972**, *76*, 3287. (b) Moynihan, C. T.; Balitactac, N.; Boone, L.; Litovitz, T. A. *J. Chem. Phys.* **1971**, *55*, 3013.

(32) Oldekop, W. *Glastech Ber.* **1957**, *30*, 8.

(33) Laughlin, W. T.; Uhlmann, D. R. *J. Phys. Chem.* **1972**, *76*, 2317.

(34) (a) Angell, C. A. In *Relaxations in Complex Systems*; Ngai, K., Wright, G. B., Eds.; National Technical Information Service, U.S. Department of Commerce: Springfield, VA, 1985; p 1. (b) Angell, C. A. *J. Non-Cryst. Solids* **1991**, *131−133*, 13−31. (c) Angell, C. A. *Science* **1995**, *267*, 1924.

(35) Alba, C.; Busse, L. E.; Angell, C. A. *J. Chem. Phys.* **1990**, *92*, 617.

(36) Wang, L.-M.; Angell, C. A. *J. Chem. Phys.* **2002**, *117*, 10184.

(37) Duvvuri, K.; Richert, R. *J. Chem. Phys.* **2002**, *117*, 4414.

(38) Yang, M.; Richert, R. *Chem. Phys.* **2002**, *284*, 103.

(39) Angell, C. A.; Imrie, C. T.; Ingram, M. D. *Polym. Int.* **1998**, *47*, 9.

(40) Yoshizawa, M.; Xu, W.; Hayashi, A.; Angell, C. A., to be published.

(41) Angell, C. A.; Xu, W.; Yoshizawa, M.; Hayashi, A.; Belieres, J.-P. In *Ionic Liquids: The Front and Future of Material Development* (in Jpn.); Ohno, H., Ed.; High Technology Information: Tokyo, 2003, pp 43−55. (English version is available from the corresponding author upon request.)

(42) Walden, P. *Z. Phys. Chem.* **1906**, *55*, 207 and 246.

(43) Bockris, J. O'M.; Hooper, G. W. *Discuss. Faraday Soc.* **1962**, *32*, 218.

(44) This also means that the Nernst−Einstein equation[45] that connects self-diffusivity to partial equivalent conductivity for a species i, $\lambda_i = RTz_iD_i/F^2$ (eq 3) (where z_i is the ionic charge and F is the Faraday), will apply when appropriate allowance is made for the friction exerted by the positive-ion flow on the oppositely directed negative-ion flow. This friction effect is zero in the ideally *dilute* solutions for which the Nernst−Einstein equation is derived but is quite large (>30%) for concentrated aqueous solutions and molten salts,[45,46] which are not usually thought of as associated liquids. Interestingly enough, MacFarlane and co-workers[47] have shown that eq 3 describes, within some 20%, the relation between conductivity and diffusivity in mixed-anion systems with imidazolium-type cations, which suggests that the interionic electrochemical friction may dissipate with increasing ionic size.

(45) Bockris, J. O'M.; Reddy, A. K. N. *Modern Electrochemistry*, Plenum Press: New York and London, 2nd Ed., 1998.

(46) Videa, M.; Xu, W.; Geil, B.; Marzke, R.; Angell, C. A. *J. Electrochem. Soc.* **2000**, *148*, A1352.

(47) Every, H.; Bishop, A. G.; Forsyth, M.; MacFarlane, D. R. *Electrochim. Acta* **2000**, *45*, 1279.

(48) McLin, M. G.; Angell, C. A. *J. Phys. Chem.* **1991**, *95*, 9464.

(49) Yoshizawa, M.; Xu, W.; Angell, C. A., submitted to *J. Am. Chem. Soc.*

(50) Janz, G. J. *J. Phys. Chem. Ref. Data* **1988**, *17*(2). ("Thermodynamic and Transport Properties for Molten Salts: Correlation Equations for Critically Evaluated Density, Surface Tension, Electrical Conductance, and Viscosity Data".)

(51) (a) McLin, M.; Angell, C. A. *J. Phys. Chem. B* **1988**, *92*, 2083. (b) Videa, M.; Angell, C. A. *J. Phys. Chem. B* **1999**, *103*, 4185.

(52) (a) Biltz, W.; Klemm, W. *Z. Anorg. Allg. Chem.* **1926**, *152*, 267. (b) Pugsley, F. A.; Westmore, F. E. W. *Can. J. Chem.* **1954**, *32*, 839.

(53) Every, H. A.; Bishop, A. G.; MacFarlane, D. R.; Oradd, G.; Forsyth, M.; *J. Mater. Chem.* **2001**, *11*, 3031.

(54) Adam, G.; Gibbs, J. H. *J. Chem. Phys.* **1965**, *43*, 139. (b) Cohen, M. H.; Turnbull, D. *J. Chem. Phys.* **1959**, *31*, 1164.

(55) Angell, C. A.; Helphrey, D. B. *J. Phys. Chem.* **1971**, *75*, 2306.

(56) Evans, D. F.; Yamauchi, A.; Roman, R.; Casassa, E. Z. *J. Colloid Interface Sci.* **1982**, *788*, 89.

(57) Xu, W.; Angell, C. A., to be published.

(58) MacFarlane, D. R.; Golding, J.; Forsyth, S.; Forsyth, M. *Chem. Commun. (Cambridge, U.K.)* **2001**, *16*, 1430.

(59) See ref 23, section 4.4.

(60) Angell, C. A.; Liu, C.; Sanchez, E. *Nature* **1993**, *362*, 137.